PHYSICAL REVIEW E **68**, 041708 (2003)

Thermal and optical study of the kinetics of the nematic-isotropic transition in octylcyanobiphenyl

F. Mercuri, U. Zammit, F. Scudieri, and M. Marinelli
Dipartimento de Meccanica, Università di Roma "Tor Vergata" and Sez. Roma II INFM, Roma, Italy

(Received 24 July 2003; published 27 October 2003)

It is shown in this paper that the kinetics of the nematic-isotropic (NI) transition in 30-μm-thick octylcyanobiphenyl liquid crystal films is strongly affected by the cell walls. We have found that this is due to the modification of the wetting properties of the liquid crystal depending on the surface treatment. The results have been obtained with an experimental setup which allows the simultaneous high resolution study of the sample thermal properties and texture evolution with temperature. An accurate determination of the width of the two phase coexistence region associated with the NI transition has been possible and it is shown that it is affected by the presence of a surfactant. The results have been interpreted with a simple model which is based on the possible presence of a well-defined interface between the nematic and the isotropic phases in the coexistence region, which depends not only on the thermal gradients in the sample but also on the surface treatments.

DOI: 10.1103/PhysRevE.68.041708 PACS number(s): 64.70.Md, 78.20.Nv

I. INTRODUCTION

The nematic-isotropic (NI) transition is known to be a weak first-order phase transition in octylcyanobiphenyl (8CB) liquid crystal (LC) as can be deduced by its quite small latent heat of (612 ± 5) J/mol [1].This is a serious complication in the study of the transition itself and, in particular, in the study of the critical phenomena associated with it, both from the theoretical and the experimental point of view. The main problem in the first case is that we have models for second-order transitions only. They have been adjusted to be used with the NI transition also but, although some progress has recently been made [2], there are some aspects still far from being fully understood. However, the so-called tricritical hypothesis [3], which had been formulated years ago, seems to have been confirmed by the available experimental data [4]. From the experimental point of view, the main drawback is the existence of a two phase coexistence region (TPCR), which is always present in the vicinity of a first-order phase transition. In other words, we do not have a single transition temperature as expected in ideal systems, but a temperature range across the phase transition in which the two phases coexist. The data in the TPCR cannot be used in the study of critical phenomena, and most of the time they are simply skipped because of the difficulty in deriving from them any useful information on the behavior of physical quantities close to T_{NI} for a two phase system. The extent of the TPCR should thus be reduced to a minimum. Also, in the case in which it is reasonably easy to overcome this problem, the fact that the kinetics of the transition and therefore the temperature evolution of one phase into the other is dependent on the experimental conditions makes the solution of this problem very difficult. It has been suggested [5], in fact, that the specific heat in the TPCR has an imaginary part and therefore is frequency dependent in ac calorimetric measurements, because of the partial conversion between the two phases in a heating cycle.

The issues we have tried to address in this paper are essentially two: the first is if it is possible to find a relation between the kinetics of the NI transition and the experimental conditions in LC films tens of microns thick and the second is if, by using ac high resolution photothermal calorimetry, it is possible to obtain information about this kinetics together with an accurate determination of the width of the TPCR and of other experimental parameters governing the TCPR.

Concerning the first issue there are many data available in the literature regarding the kinetics of first-order transitions in thermal quenches [6], but almost no data in systems at thermodynamic equilibrium. The situation is completely different in the two cases and it is not possible to extrapolate the results obtained in the first case to the second, because of the strong undercooling required for the quenching which conflicts with the quasiadiabatic equilibrium needed in high resolution phase transition studies. Another important aspect concerning the kinetics of the NI transition is the possible influence of surfaces in relatively thick films such as the ones considered in this study. We have quite a lot of information on the influence of surfaces on phase transitions in nanometer thick films [7] but not very many data on what could be their role, if there is any, in rather thicker samples. Cell walls are often treated to induce macroscopic alignment in LC and it could be interesting to know whether these treatments influence the kinetics of the transition or not.

Concerning the second issue, a model for the behavior of the photothermal signal in ac photothermal calorimeters at first-order phase transitions had been proposed about two decades ago [8]. The model is based on the assumption that an interface separating the two phases is present in the TPCR and describes the contribution to the signal due the oscillation of the interface position in the sample because of the ac heat input. In high resolution measurements, however, the temperature oscillation introduced in the sample by the measuring technique, and therefore the oscillation of the interface, must be minimized and it is not clear if the proposed mechanism is still valid. Moreover there is no experimental evidence of the presence of such an interface in the TPCR.

In this paper we report on the results obtained with an experimental apparatus [9] that allows the simultaneous high resolution study of thermal parameters and of the sample texture evolution with temperature at the same time. Specific heat, thermal conductivity, and thermal diffusivity data have been obtained with an ac photopyroelectric calorimeter in which polarizing microscopy was implemented. We have studied samples with different cell wall surface treatments. These are samples with no treatment, with surface deposition of thin quartz layers at grazing angle and of the polar surfactant cetyl trimethylammoniumbromide (CTAB) so as to induce in the last two cases planar and homeotropic alignments of the samples, respectively. We have found that the kinetics of the transition in the first two cases is very similar but different when heating or cooling the samples. In the case of samples treated with CTAB we have found, however, that the kinetics upon heating or cooling the sample is reversed with respect to previous two cases and that it is similar to those obtained when cooling or heating, respectively, the the previous two samples. This behavior is attributed to the different wetting properties of the material at the cell walls which influence the nucleation of one phase into the other. We have also found that the presence of CTAB increases the width of the TPCR with respect to the other two cases in which the width is practically the same.

The difference in the kinetics, when heating or cooling the sample, has been attributed to the fact that, as confirmed by texture analysis, a well-defined interface between the nematic (N) and isotropic (I) phases in the TPCR may or may not be formed in the sample depending on the conditions. This is not only due to the presence of thermal gradient in the samples but also due to the wetting property at the sample cell walls, which in turn depends on their treatment and on the starting phase of the transition. We have compared these conclusions, derived by the experimental results, with a simple model for the generation of the photopyroelectric signal (PPE) in our calorimeter. The model is based on the contribution to the PPE signal of the thermal wave reflected at the NI interface when this is present. We have performed some simulations, reproducing reasonably well the experimental data, which are not consistent with the oscillating interface model mentioned above [8].

Finally, we do not find any evidence in our samples of a partial conversion of one phase into the other during one heating cycle in the TPCR [5] which can originate a frequency dependent specific heat at the NI transition in 8CB.

II. EXPERIMENT

The experimental apparatus we have used in this work combines the capabilities of a high resolution ac photopyroelectric calorimeter and those of polarizing microscopy. We have used a standard back detection (BD) configuration by which the specific heat c, the thermal conductivity k, and the thermal diffusivity D of the sample can be determined [10], and the front detection (FD) one in which only the sample effusivity ($e_s = \sqrt{k\rho c}$, where ρ is the sample density) can be derived [11]. In both cases the sample cell thickness was 30 μm and the modulation frequency was 81 Hz, apart from some measurements in FD configuration in which it was 720 Hz. At these frequencies the samples are thermally thick (sample thickness l much larger than the thermal diffusion length $l_T = \sqrt{D/\pi f}$, where f is the modulation frequency). The heating source was an acoustoptically modulated 5-mW He-Ne laser. The pyroelectric transducer, a 300-μm-thick $LiTaO_3$ crystal, was used as a cover for the cell and one of its electrodes was in contact with the LC. In BD configuration we have used pyros with indium-tin-oxide (ITO) transparent electrodes and the laser light was absorbed by a thin (200 nm) Ti layer deposited on the cell surface in contact with the liquid crystal. This metallic layer is opaque to visible light and generates heat at the LC surface opposite to the one in contact with the pyroelectric transducer. Moreover, it is also thermally thin and does not affect the heat diffusion process. The optical access provided by the transparent electrodes allowed polarizing microscopy, with the light of a low power lamp reflected at the Ti layer after having crossed the sample. The lamp power was reduced to make the possible thermal gradient induced in the sample negligible. In FD we have used pyros with one ITO transparent electrode while the other, in contact with the LC, was a thin (about 200 nm) gold layer. The ac laser light was impinging on the pyro on the transparent electrode side and absorbed at the gold one. Heat is generated at the LC surface and the temperature oscillation detected at the same surface. The cell was completely transparent, and allowed optical access to the sample from the cell side, with the light of the lamp reflected in this case at the gold electrode of the pyro. The microscope was equipped with a charge-coupled device (CCD) camera which allowed texture analysis of the sample during the measurement. The sample plus pyro assembly was contained in an oven and the temperature rate change during the measurement was 1 mK/min.

III. RESULTS

A. Sample alignment

One of the main aims of this paper is the study of the influence of surfaces on the kinetics of phase transitions of few tens of micrometer thick LC layers and we have therefore preliminarily studied their effect on the sample ordering. Three different types of samples have been prepared: in the first case (type A) a very thin layer of quartz has been sputtered at grazing angle on the cell walls, in the second (type B) the surfaces have been treated with a surfactant (1% in weight CTAB in chloroform), and in the third (type C) the surfaces were not treated. We have performed a conoscopic analysis of the samples and, as expected, we have found that type A and type B showed planar and homeotropic alignments, respectively. Type C samples were also found to be homeotropic but polarizing microscopy showed that while type B were monodomain samples, in type C samples small areas with random orientational defects were present (Fig. 1).

Figure 2 shows the thermal diffusivity data obtained in the three different cases described above. The thermal diffusivity ($D = k/\rho c$, where k is the thermal conductivity, ρ is the sample density, and c is the specific heat) is an indicator of the sample alignment [12]: the larger (the smaller) the value in the ordered phases, the higher the degree of homeotropic (planar) alignment. This is clearly shown in Fig. 2 where type A sample, which exhibits a planar alignment, has D values in the ordered phases much smaller than type B

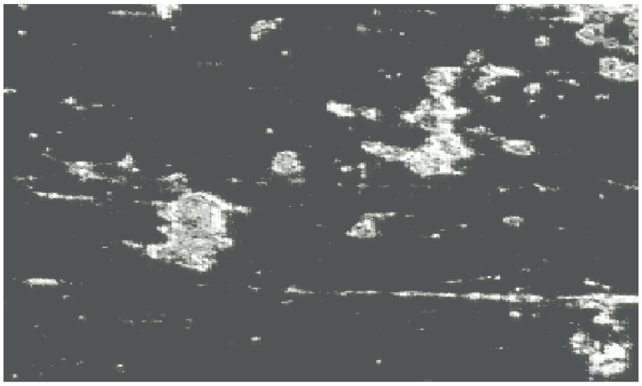

FIG. 1. Polarizing microscopy image of type *C* sample.

sample which is homeotropic. *D* values for type *C* sample are not very different from those obtained for type *B* and it can be therefore concluded that, in agreement with conoscopic images, the alignment is homeotropic. The alignment quality, however, is not as good as for type *B*, which has a larger value of *D* at all temperatures in the ordered phases, due to the presence of the defects in type *C* sample as shown in Fig. 1(b).

B. Front detection

1. Type A sample

Figure 3 shows the amplitude and the phase of the PPE signal obtained on heating (a) and on cooling (b). It must be noted that raw data are reported in the figure and that the noise is remarkably small ($\leqslant 0.03°$ in the phase) for a signal amplitude of only a few tens of microvolts.

In front detection configuration, provided that the sample is homogeneous (monophasic), optically opaque, and thermally thick, the amplitude and the phase of the PPE signal are given by [11]

$$A\propto \frac{1}{\frac{e_s}{e_p}+1}, \qquad \phi=\text{const}, \tag{1}$$

where $e_i=\sqrt{(k\rho c)_i}$ is the thermal effusivity, with $i=s,p$ corresponding to the sample and the pyro, respectively.

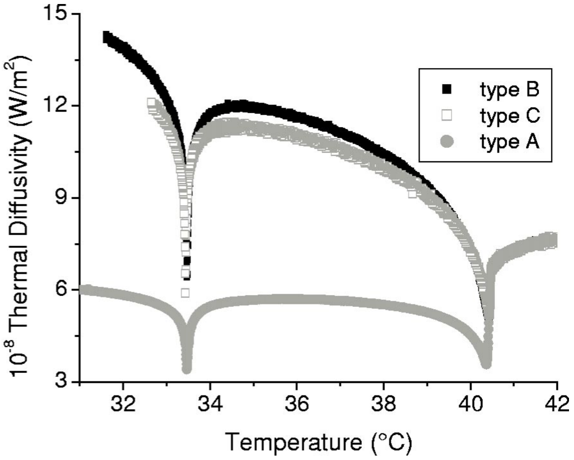

FIG. 2. Thermal diffusivity for type *A*, *B*, and *C* samples vs temperature.

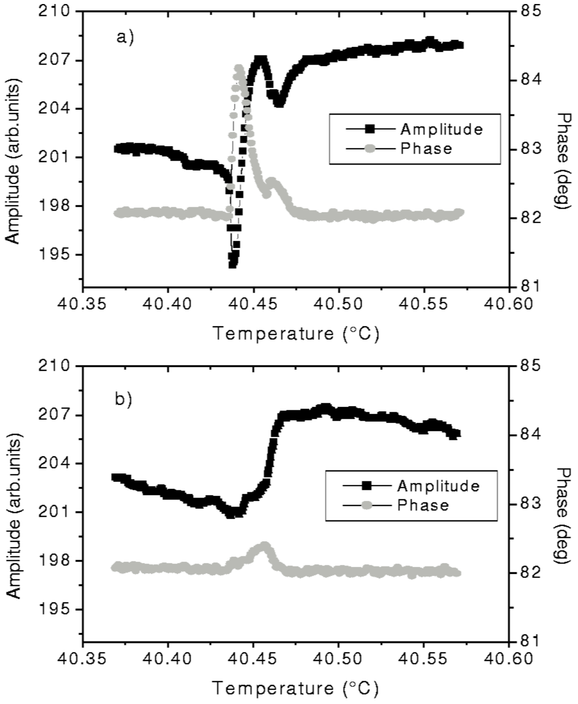

FIG. 3. Amplitude and phase of the PPE signal for type *A* sample on (a) heating and (b) cooling in FD configuration.

In Fig. 3(a) the phase is almost constant for $T_{1A} < 40.435$ mK and $T_{2A} > 40.475$ mK, but it shows a double peak structure for $T_{1A} < T < T_{2A}$ and therefore in the NI transition region. This means that one or more of the conditions for the validity of the results in Eq. (1) is not fulfilled close to T_{NI}. This is also true for the amplitude, whose behavior is consistent with the variation of the thermal effusivity e_s (e_p is constant in the temperature range of the measurements) away from T_{NI} and shows a peak, close to T_{NI}, at a slightly higher temperature with respect to the sharpest one in the phase.

It is well known that the NI is a weak first-order phase transition [1]. In ideal samples, with no thermal gradients, and with no defects and pollutants in it, there is one single temperature T_{NI} at which the nematic and the isotropic phases coexist. For $T < T_{NI}$ the sample is completely nematic and it is isotropic for $T > T_{NI}$. In real samples, however, even in the high purity ones, we always have pollutants and defects which can act as nucleation centers for one phase within the second one even at a temperature different from T_{NI}. Moreover unwanted imperfection in the heating stage and the measuring technique itself can induce temperature gradients in the sample. We have, therefore, different parts of the sample at different temperatures undergoing a phase transition not at the same time. The result is that, instead of a single transition temperature, we have a TPCR, whose width can be reduced improving the sample purity and reducing as much as possible the thermal gradients in the sample. As a consequence, the sample is not thermally homogeneous in the TPCR, since the N and I phases have different thermal

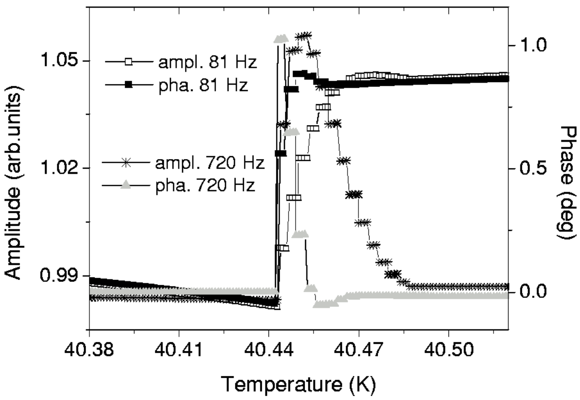

FIG. 4. Simulation of the PPE amplitude and phase vs temperature in FD configuration close to T_{NI}.

properties, and the results in Eq. (1) do not therefore apply.

The above conclusion does not explain, however, the observed behavior for the phase and the amplitude [Fig. 3(a)].

A possible explanation for the obtained results could be the following. Ac heating produces highly damped thermal waves which propagate into the sample. Let us imagine that, because of the dc component of the temperature rise produced by the ac heating source, a vertical gradient, perpendicular to the surfaces, is established in the sample. At a certain temperature, when heating the sample the I phase starts to nucleate at the surface where the heat is generated, which is at higher temperature with respect to the opposite one because of the above mentioned gradient. An interface between the I and N phases is therefore established and a further increase of the ambient temperature moves the interface toward the low temperature side of the sample. Because of the discontinuity of the thermal parameters across the interface, the thermal wave generated at the heated surface is reflected at the interface [13]. The reflected wave propagates back to the heated surface, where, in FD, the pyro signal is detected, and contributes to its temperature rise.

To see if the above mentioned hypothesis is consistent with our results, we have performed some calculations whose results are reported in Fig. 4. We have derived the PPE signal amplitude and phase for a 8CB LC sample from the temperature rise induced at the heated surface by numerically solving the one-dimensional heat diffusion equation. We have introduced a vertical gradient of 50 mK which, combined with the ambient temperature change, induces the movement of the interface in the TPCR. For the thermal parameters vs temperature values in the N and I phases we have used the expressions obtained from the best fits obtained against the sample thermal parameters values derived from BD measurements over the NI transition (see below). The results of the calculations (Fig. 4) reproduce reasonably well the experimental behavior of the phase [Fig. 3(a)] especially if one considers that they have been obtained making two assumption not fully justified by the experimental results (see below): a well-defined interface which remains flat and parallel to sample surfaces while moving and an abrupt change of the sample thermal parameters. Increasing the temperature, the high temperature side of the sample becomes isotropic and this corresponds to a sharp increase of the phase, partly smoothed by the vertical gradient. A further increase of the temperature induces an increase and a subsequent decrease of the phase which are related to the shift of the interface away from the laser heated surface. φ becomes almost constant when the interface is at a distance greater than the thermal diffusion length from the surface.

The calculation reproduces quite well also the behavior of the amplitude, apart from a very narrow temperature region around T= 40.437 °C where it shows a sharp dip. This is due to the presence of the latent heat which is associated with the first-order NI transition and not considered in the calculations. It has been shown [8] that latent heat plays a significant role especially at the early stage of the nucleation of the high temperature phase close to the heated surface since it suppresses the temperature oscillations induced by the ac heat input. The basic mechanism is the following. Assuming that the ambient temperature is very close to T_{NI}, the ac heating source induces the nucleation of a very thin isotropic layer close to the surface with no temperature variation in it, because of the latent heat involved. The amplitude of the PPE signal, therefore, tends to zero. Increasing the ambient temperature, the NI interface, and therefore the sample region involved in the transition, shifts away from the heated surface into the sample volume. This means that the average depth of the interface, around which the interface position oscillates due to the ac heat input, increases. This oscillation, combined with the absorption and release of the latent heat, causes the temperature oscillation at the surface where the pyro detection takes place to increase again. We believe, however, that this mechanism is relevant only in the narrow temperature region close to $T = 40.437\,^{\circ}\mathrm{C}$ mentioned above, with the reflection of the thermal wave playing a major role in all the rest of the TPCR.

The video taken during the measurement provides additional evidence that the behavior of the amplitude and phase on heating in the TPCR is due to the above mentioned reflection of the thermal wave. Figure 5(a) shows an image taken at $T = 40.435\,^{\circ}\mathrm{C}$. Here the light areas correspond to nematic material both extending throughout the entire sample thickness and at the interface with isotropic material, while the dark areas correspond only to isotropic material. It is clearly evident that while the left and the right parts of the sample are fully nematic, and isotropic respectively, there is a region in the middle in which the two phases coexist. The temperature evolution of this region is consistent with the fact that a thin isotropic layer starts to nucleate at the heated surface (opposite to the one facing the CCD camera), because of the vertical temperature gradient introduced by the laser, and it progressively becomes thicker with increasing ambient temperature. Superimposed on this there is also another effect due to a spurious lateral temperature gradient (parallel to the sample surfaces), due to a nonperfect design of the heating stage, which causes the displacement of the TPCR from right to left in the image. As a result we have, in the sample region probed by the PPE measurement, a vertically moving interface in the TPCR, which is not exactly parallel to the sample surfaces and not completely flat since the nucleation of the I material is not homogeneous all across

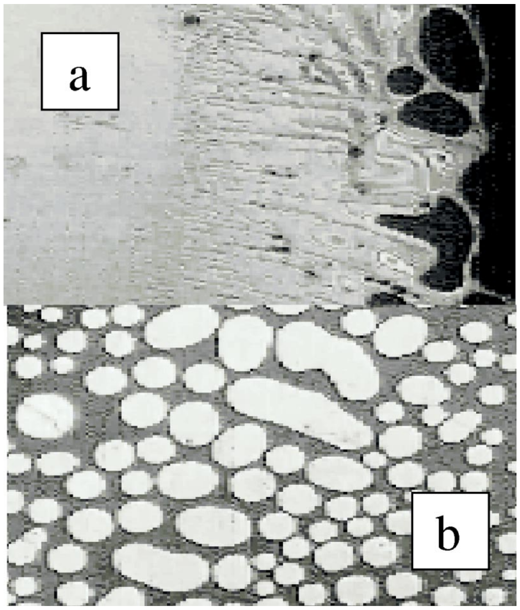

FIG. 5. Polarizing microscopy images of type A sample taken at (a) $T=40.445\,^{\circ}\mathrm{C}$ on heating and (b) $T=40.460\,^{\circ}\mathrm{C}$ on cooling.

the sample. Finally, Newton interference colors appear in a well-defined sequence as the nematic layer progressively becomes thinner with increasing ambient temperature.

From the video observation it turns out that in the region where the PPE signal is generated, which approximately corresponds to the spot size of the heating source, the onset of the TPCR is at T_{1A}; that T_{1A} corresponds to the temperature at which the amplitude and the phase start to increase in Fig. 3(a); and that for $T>T_{2A}$ the phase remains practically constant while the slight progressive increase in amplitude reflects effusivity behavior of a fully isotropic sample. We can therefore conclude that the observed texture evolution is fully consistent with the proposed explanation of the behavior of the amplitude and the phase of the PPE signal in the TPCR.

The arguments reported above account for the low temperature peak in the phase. There is, however, a second smaller peak at higher temperature in Fig. 3(a) whose origin can be explained as follows. The growth of the isotropic layer with temperature causes the movement of a NI interface from the high temperature side to the low temperature one, as stated previously. The interface is not perfectly flat and uniform and therefore when the isotropic phase reaches the low temperature side of the sample at some points, some other points are still in the nematic phase. The video clearly shows that when this happens the second smaller peak in the phase shows up. The video also shows that when the interface reaches the colder side of the sample and isolates a nematic volume within the isotropic phase, the volume immediately shrinks. This is due to the fact that the contact angle between the two phases and the substrate cannot be indefinitely small but assumes a well-defined value which depends on the surface tension. The decrease of the surface bounding the nematic volumes produces, of course, an increase in their thicknesses and a recoil of the NI interface of these volumes away from the cooler side of the sample. When this happens, the phase must increase as shown in Fig. 4.

When the sample is cooled from the isotropic phase, [Fig. 3(b)] the amplitude and the phase of the PPE signal are very different from the ones obtained when heating the sample. A single small and broad peak has been obtained for the phase and there is no peak structure on the high temperature side of the NI transition of the amplitude. According to the mechanisms proposed earlier, it means that the contribution of the reflected thermal wave is severely reduced. Figure 5(b) shows an image taken at $T=40.460\,^{\circ}\mathrm{C}$ during the measurement which shows no clear interface between the isotropic and the nematic phases. Isolated nematic volumes appear and the transition occurs via their coalescence with decreasing temperature. Contrary to what was observed when the NI interface was close to the lower temperature side of the sample, during the heating of the sample, no Newton colors are detected at the early stage of the nematic phase nucleation at the same surface. This means that the nucleated nematic volumes are rather thick, denoting a vertical temperature gradient in the sample which is smaller in this case with respect to the one obtained when heating the sample. This can be understood if one considers that in our setup, for geometrical reasons, the heat exchange of the LC cell with the ambient is slightly more efficient on the side where the ac heating source impinges. Thus, this causes an additional thermal gradient which reinforces the dc gradient introduced by the laser when heating the sample and reduces it when cooling the sample.

The absence of a well-defined interface is also the reason why we have not found the sharp dip in the amplitude found on heating when the isotropic phase becomes very thin and close to the high temperature sample surface.

Also in this case the video taken during the measurement confirms that the width of the TPCR corresponds to the temperature region where the phase substantially changes. Its value of 40 mK is very close to the one obtained when heating the sample.

2. Type B sample

Figure 6 shows the amplitude and the phase of the PPE signal upon heating (a) and cooling (b) the type *B* sample.

Upon heating no dip, close to the transition temperature, as the one observed in Fig. 3(a), has been detected in the amplitude, which starts to increase, after an initial decrease, at $T_{1B}=40.421\,^{\circ}\mathrm{C}$. At approximately the same temperature a peak starts appearing in the phase that is much less pronounced with respect to the corresponding one for sample *A*, but comparable to the one obtained for that sample upon cooling. The phase then remains fairly constant for $T>T_{2B}=40.474\,^{\circ}\mathrm{C}$ after the amplitude too has saturated to a fairly constant value.

The video shows that at T_{1B} small isotropic areas appear at the low temperature side of the sample, as shown in Fig. 7(a). Here the dark lines correspond to the NI interface. There is no contrast between the N and I areas, and this strongly suggests that they are isotropic columns in a nematic sea, whose depth is approximately equal to the sample thickness. The size of the columns increases with increasing

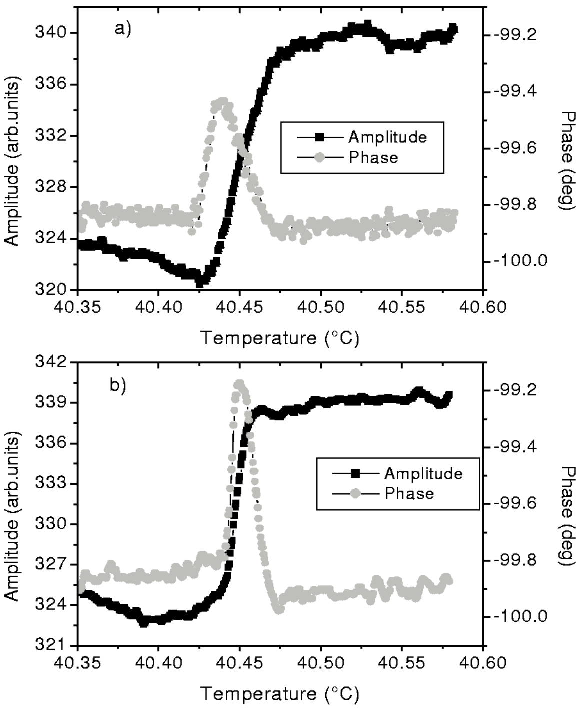

FIG. 6. Amplitude and phase of the PPE signal for type *B* sample on (a) heating and (b) cooling in FD configuration.

temperature and the transition takes place via the coalescence of the columns. The sample is completely isotropic at T_{2B}. The TPRC is in this case 53 mK, larger than the one obtained in type *A* samples.

There are close similarities between these results and the ones obtained when cooling the type *A* sample, and this is essentially due to the lack of a well-defined interface between the N and I phases for both cases. The height of the peak in the phase is in fact approximately the same in the two cases and the amplitude does not show any dip at the early stage of the isotropic phase nucleation. The only difference is in the alignment of the molecules (homeotropic in this case and planar in sample *A*) which has an effect on the values of the sample thermal conductivity and the thermal diffusivity, and on the sample optical activity which affects the contrast (color) in the polarizing microscopy images [see Figs. 5(b) and 7(a)].

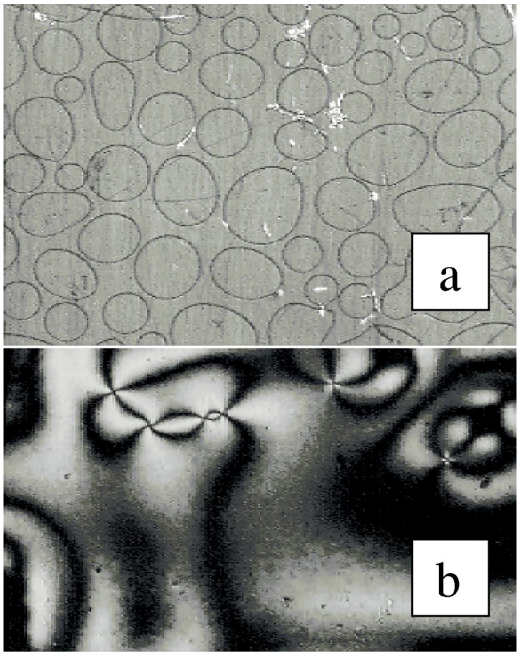

FIG. 7. Polarizing microscopy images of type *A* sample taken at (a) $T=40.450$ °C on heating and (b) $T=40.460$ °C on cooling.

When cooling the sample, [Fig. 6(b)] the amplitude starts to decrease at $T=40.461$ °C, where the bright areas corresponding to nematic thin layers appear on the low temperature side of the sample. When the temperature is decreased, the video shows that the bright areas form a uniform texture which changes its color (increases its thickness), and reaches the opposite side of the sample in some points at $T=40.449$ °C, where the phase reaches its maximum, before the appearance of a fully nematic layer. A typical texture in the vicinity of $T=40.458$ °C is shown in Fig. 7(b), where some hedgehog defects are also present. This texture evolution can be explained as follows [9]. Isotropic thin layers nucleate on one side of the sample. The LC molecules are oriented at the NI interface along a direction that forms an angle of 63° with respect to the normal to the interface [14]. Because of the homeotropic alignment of the molecules at the surface where the nucleation starts, the fraction of the sample which is in the nematic phase has a hybrid alignment and therefore appears bright between crossed polarizers. Newton interference is observed in the layer because of sample birefringence. Decreasing the temperature, the nematic layer becomes progressively thicker and a well-defined color sequence is observed, which is reversed with respect to the one obtained when heating type *A* sample. This is obviously due to the fact that in that case the nematic layer thickness was decreasing with increasing temperature. After a steep decrease the amplitude saturates at $T=40.392$ °C, where the sample is fully nematic. At $T=40.449$ °C, where the phase reaches its maximum, the nematic film reaches the opposite side of the sample and a further decrease in temperature produces a decrease in the phase, which becomes almost constant for $T\leqslant 40.392$ °C. In such a temperature range only very tiny isotropic layers are left and they eventually disappear at approximately the same temperature at which the amplitude starts to increase again after its steep decrease over the transition region. These residual volumes are responsible for the broadening of the dip with respect to the one obtained on heating. The width of the TPCR in this case is 70 mK, which is larger than the one obtained on heating the sample and also than the one obtained in type *A* samples.

The described behavior of the PPE signal amplitude and phase is qualitatively similar to one obtained for type *A* sample on heating. Again, this is due to the fact that in both cases there is an interface between the N and I phases. Nevertheless, the height of the peak in the phase is much smaller than the corresponding one shown in Fig. 3(a). This can be related to the relatively large density of hedgehog defects shown in Fig. 7(b) which are typical of a nematic. These

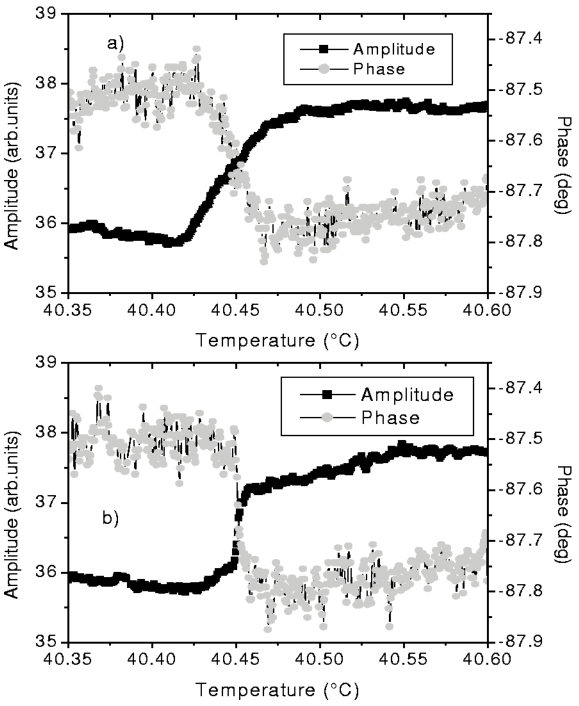

FIG. 8. Amplitude and phase of the PPE signal for type *B* sample on (a) heating and (b) cooling in FD configuration at 720 Hz.

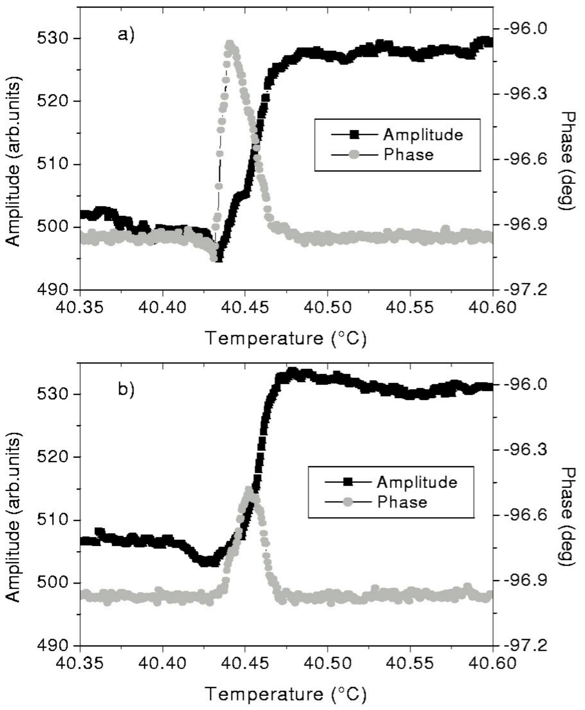

FIG. 9. Amplitude and phase of the PPE signal for type *C* sample on (a) heating and (b) cooling in FD configuration.

defects can affect the orientation of the molecules at the NI interface, with a smearing of the discontinuity of the thermal parameters responsible for the thermal wave reflection. This can also be the reason why we do not see any peak structure in the amplitude on the high temperature side of the transition as in the case of type *A* samples.

To check further the validity of our hypothesis which explains the observed behavior of the amplitude and phase in TPCR in terms of a reflection of the thermal wave, we have increased the frequency to 720 Hz in some experiments on type *B* samples. The results are shown in Fig. 8 when heating the sample (a) and when cooling it (b). The amplitudes are qualitatively similar to the ones obtained at 81 Hz. The phase behavior is, on the other hand, remarkably different with respect to the corresponding one at 81 Hz, since no peaks are detected either upon heating or upon cooling the sample. This can be understood if we go back to Fig. 4 where the calculations for 720 Hz are also shown. It turns out that with such a frequency increase the width of the temperature region corresponding to the peak in the phase is reduced by approximately a factor of 3. The thermal diffusion length μ, in fact, decreases with frequency and since the contribution of the reflected thermal wave to the PPE signal depends on the depth of the interface with respect to the μ, this implies a decrease of the temperature range in which such a contribution is relevant due to the NI interface shifting deeper into the sample with increasing ambient temperature. As it turns out the factor 9 in the frequency increase corresponds to a factor of 3 in the decrease of the thermal diffusion length. A reduction in the observed region where the phase shows a substantial variation is also evident in the experimental data of Fig. 8(b) with respect to the data reported in Fig. 6(b), and this is for the cooling run where the peak in the phase should have been more prominent. So, it may well be that the peak in the phase cannot be experimentally detected because of such a reduced width of the transition region [only about 10 mK in Fig. 8(b)] which can cause the structure to be smeared out by the temperature gradient. Moreover, the noise level in the phase has now increased due to the reduction of the PPE signal level. This too may contribute to the smearing of the expected structure in the phase. The trend which shows a decrease of the width of the peak with increasing frequency, confirmed by the experiments, is a further evidence supporting the validity of the proposed explanation of the behavior of the PPE signal amplitude and phase in the TPCR.

We have also performed some measurements increasing the power of the heating source to increase the vertical gradient in the sample. The results we have obtained (not shown) show an increase of the peak in the phase. This is due to the fact that the larger thermal gradient enforces the formation of the interface and, in agreement with the proposed scenario, the contribution of the reflected thermal wave to the surface temperature oscillation is also increased. The width of the TPCR is, of course, increased in this set of experiments.

3. Type C sample

The results obtained in this case for the PPE signal and phase are shown in Fig. 9 when heating (a) and cooling (b) the sample *C*.

In the heating run the amplitude and the phase show a temperature dependence qualitatively similar to the one found for type *A* samples. The main difference in the phase consists in the presence of a less pronounced peak, while the

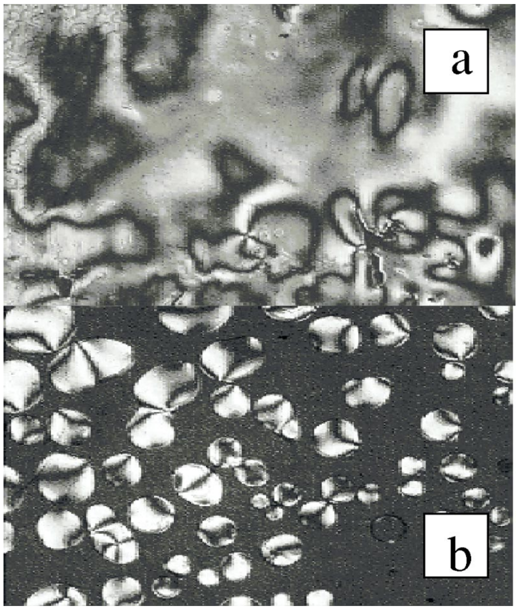

FIG. 10. Polarizing microscopy images of type *A* sample taken at (a) $T=40.447\,°\mathrm{C}$ on heating and (b) $T=40.463\ °\mathrm{C}$ on cooling.

amplitude shows no peak on the high temperature side of the transition and a shallow dip on the low temperature side.

The video recorded during this measurement confirms the above mentioned similarity. It shows a texture evolution consistent with the formation on an isotropic layer at the high temperature sample surface, at the temperature where the amplitude has the dip, and a NI interface that moves toward the lower temperature side of the sample with increasing temperature. However, the NI interface in this case is not so well defined as in type *A* samples. This explains the reduced height of the peak in the phase and the shallower dip in the amplitude at T_{NI} also. The reason for this could be the presence of defects in the material due to the poorer alignment quality with respect to type *A* samples, as shown in Fig. 1. Moreover there is no side peak in the phase as the one on the high temperature side of the transition in type *A* samples. This side peak was attributed to residual isolated nematic volumes at the low temperature sample surface which shrink and increase their thickness when the NI interface toucher the surface at some particular points. The reason why we do not see a similar effect in this case is not fully understood, but we believe that it is related to the wetting properties of the sample at the differently treated cell walls. It should be noted, in fact, that in this case the LC is in contact with a gold layer, while in the case of type *A* samples, it is in contact with the sputtered quartz needed for the planar alignment. Finally, when the nematic layer becomes sufficiently thin, the video shows a Newton color sequence similar to the one found in type *A* samples. A typical sample texture, at $T=40.447\,°\mathrm{C}$, is shown in Fig. 10(a). The width of the TPCR turns out to be 44 mK, which is comparable to the one obtained in type *A* samples and therefore smaller than the one found in type *B* ones.

The similarity with type *A* sample also apply on cooling type *C* sample [Fig. 9(b)]. Again, no clear NI interface is detected in the video of the measurement. The phase starts to increase at $T=40.470\,°\mathrm{C}$ and shows a peak less pronounced than the one obtained when heating the sample but comparable with the one obtained when cooling type *A* sample. The video shows that at the same temperature where the phase starts to increase and the amplitude starts to decrease, small and bright areas appear. The lack of Newton colors suggests that their thickness is quite large if compared with the sample thickness. They grow in size and coalesce with decreasing temperature, and fully nematic regions appear at $T=40.425\,°\mathrm{C}$. A typical sample texture at a temperature close to $T=40.463\,°\mathrm{C}$ is shown in Fig. 10(b). The width of the TPCR is therefore 45 mK.

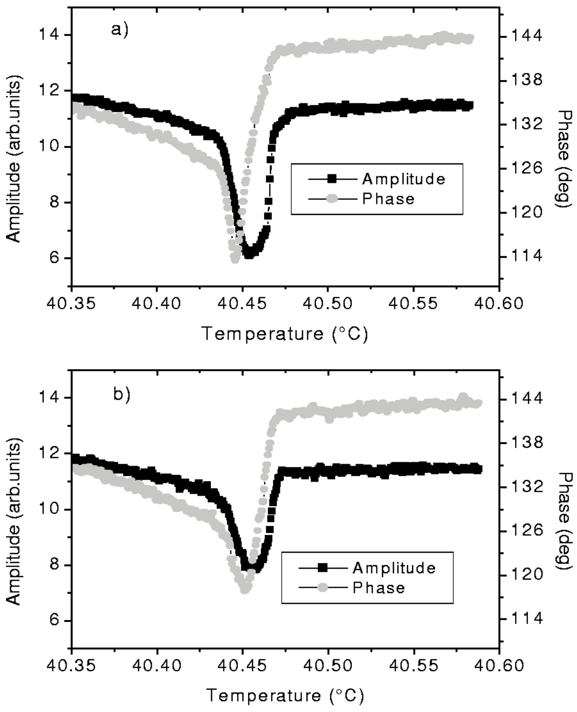

FIG. 11. Amplitude and phase of the PPE signal for type *C* sample on (a) heating and (b) cooling in BD configuration.

C. Back detection

1. Type C sample

Figure 11(a) shows the amplitude and the phase of the PPE signal in the BD configuration when heating a type *C* sample (nonaligned). Increasing the ambient temperature a drastic change in slope of the decreasing amplitude phase occurs at $T=40.433\,°\mathrm{C}$. At the same temperature, the video, which is obviously similar to the one recorded in FD for type *C* samples, shows the appearance of NI coexistence. The sample becomes fully isotropic at $T=40.473\,°\mathrm{C}$ and the width of the TPCR is therefore 40 mK, as also determined by FD detection measurements. From the results obtained in FD, one can deduce that the sharp dips in the amplitude and phase, corresponding to the presence of the TPCR, are due to presence of the interface and therefore to the contribution of the reflected thermal wave. We have performed a simulation similar to the one described earlier, this time calculating the

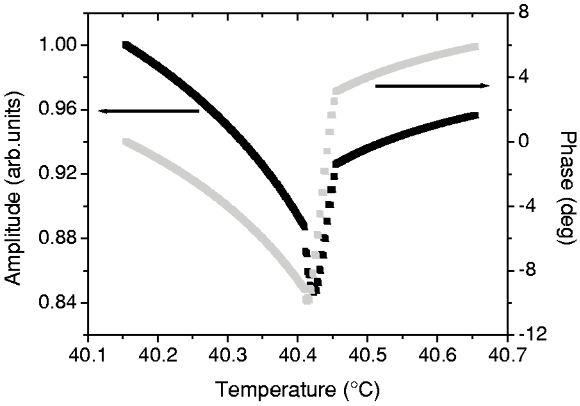

FIG. 12. Simulation of the PPE amplitude and phase vs temperature in BD configuration close to T_{NI}.

temperature oscillation induced by the heating source on the side opposite to the heated one as is the case for back detection. The results are shown in Fig. 12 and it shows an abrupt dip in the amplitude in the TPCR similar to the one found in the experiment. The phase shows a small discontinuity at the onset of the TPCR with a dip which is much smaller than the one observed for the amplitude. Also in the experimental data the phase has a smaller dip with respect to the amplitude but not as small as the one obtained in the calculations. Considering that the simplicity of the model adopted for the simulation does not allow a complete description of the real situation, we can conclude that the simulation reproduces reasonably well, at least qualitatively, the main features of the experimental results, therefore supporting the hypothesis that also in BD the behavior of amplitude and phase are related to the reflection of the thermal wave at the NI interface.

Figure 11(b) shows the results obtained for the same sample on cooling. The dips in the amplitude and phase are somewhat broader and less pronounced with respect to the ones obtained on heating and this is due to the lack of a well-defined interface as shown by the video recorded during the measurement. The width of the TPCR turns out to be 42 mK in this case, consistent with FD measurements.

Figures 13(a) and 13(b) show the amplitude and the phase in BD for a type *B* sample (homeotropic). Also in this case we have dips in the amplitude both on heating and on cooling which are broader than the corresponding ones found in type *C* sample. The width of the TPCR was found to be consistent with the one found by FD measurements and reported earlier, and is greater with respect to type *C* sample. There is practically no abrupt dip in the phase in the cooling run and again this is due to the distortion of the interface induced by hedgehog defects at the heated surface, as described previously.

The results for type *A* samples (not shown) are very similar to the ones already reported in Ref. [16] and the width of the two phase coexistence region is in agreement with FD measurements.

2. Thermal parameters

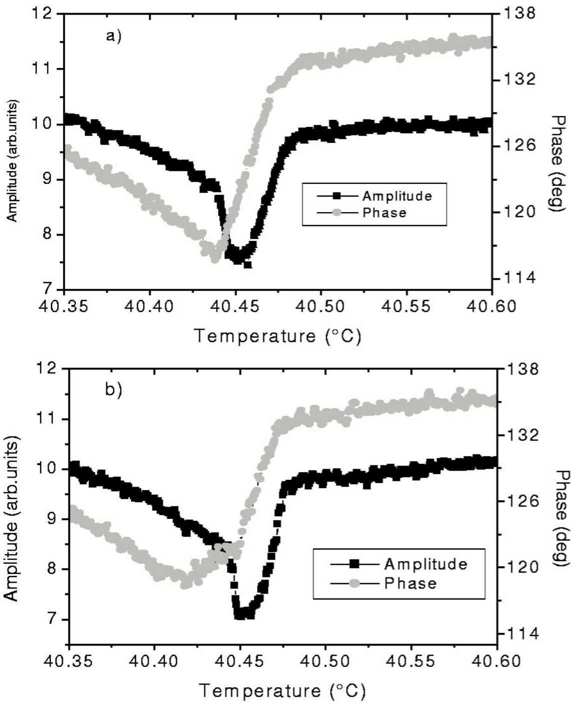

FIG. 13. Amplitude and phase of the PPE signal for type *B* sample on (a) heating and (b) cooling in BD configuration.

In the temperature region outside the TPCR the samples are thermally homogeneous, optically opaque, and thermally thick. In that region we can therefore work out the sample thermal effusivity and thermal diffusivity, from the following amplitude and phase expressions [15]:

$$A \propto \frac{1}{f}\frac{e_p}{(e_s+e_m)}\frac{\exp(-\sqrt{\pi f/D}l)}{(e_p/e_s)+1}, \qquad \varphi=-\sqrt{\pi f/D}l, \qquad (2)$$

where e_m is the known thermal effusivity of the cell material.

From these two quantities and knowing the sample density ρ we can calculate the specific heat and the thermal conductivity from the relations

$$k=e_s\sqrt{D_s}, \qquad c=\frac{1}{\rho}\left(\frac{e_s}{D_s}\right). \qquad (3)$$

The results are shown in Fig. 14. It has been shown [16] that the different alignment in 8CB does not affect the critical behavior of the thermal parameters and, since from the point of view of the width of the TPCR samples *A* and *C* are quite similar, we have decided to compare the results relative to type *B* and *C* samples only.

We have skipped in the figures the data in the TPCR whose width has been experimentally determined as described above. In all cases the curves almost overlap outside the TPCR. The specific heat data are in excellent agreement with the ones reported in Ref. [1], which have been obtained with adiabatic scanning calorimetry with a TPCR about 14 mK wide. The thermal conductivity and the thermal diffusivity are also in very good agreement with previously reported results obtained with PPE [12]. A small discontinuity is present in *k*, which does not show any critical behavior at T_{NI}. We can therefore conclude that also in this case, as in

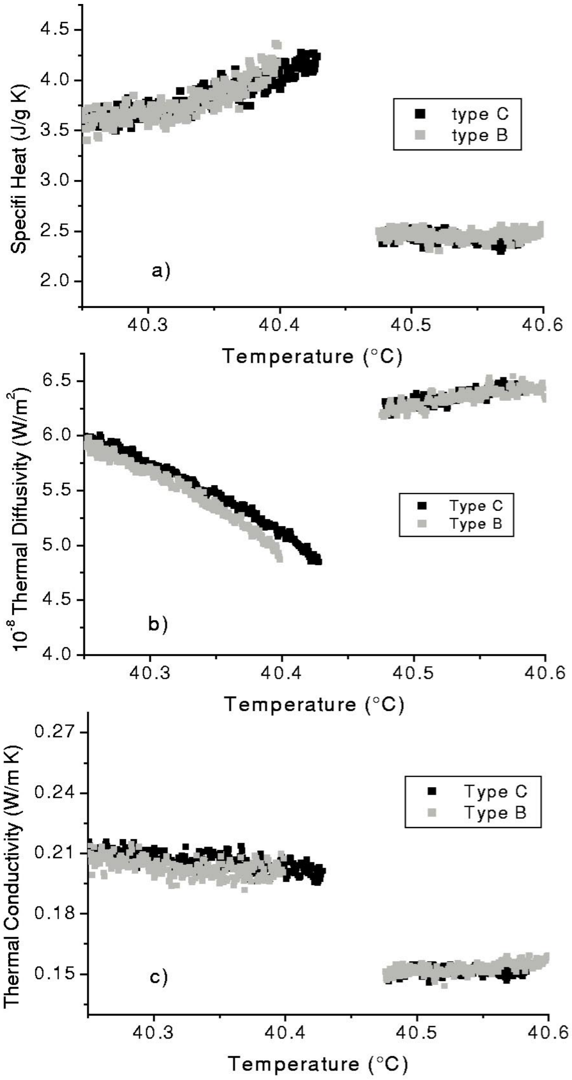

FIG. 14. Specific heat, thermal diffusivity, and thermal conductivity vs temperature for type *B* and *C* samples.

the case of the smectic A–nematic phase transition, the thermal conductivity is dominated by short range processes and therefore not affected by collective phenomena. As a consequence, the critical behavior of the thermal diffusivity is only related to that of the specific heat.

In this work we were mainly interested in the kinetics of the NI transition in the TPCR and the data were therefore collected in a very narrow region around T_{NI}. We have made some runs, using type *C* samples, scanning the temperature on a wider temperature region and the data (not shown) have been fitted to analyze the critical behavior of the specific heat. The results we have obtained confirm the tricritcal-like behavior of the transition with the critical exponent $\alpha = 0.5$. A detailed analysis of this aspect will be reported elsewhere.

IV. DISCUSSION

The results reported earlier do show that the kinetics of the NI phase transition in 8CB is largely dependent on the formation of a well-defined interface between the N and I phases in the TPCR of the sample. It should be noted that, even for an ideal sample with no defects and pollutants and for an ideal measuring setup, a NI interface must always be present when an ac calorimetric technique because of the dc temperature gradient introduced by the ac heating source. This of course is not true in high resolution dc techniques, such as the adiabatic scanning calorimetry, which however do not allow the simultaneous measurements of transport properties such as the thermal conductivity and the thermal diffusivity together with the specific heat. Our results show that the presence of the NI interface in experimental situations depends on some other factors and, in particular, on the presence of defects and on the sample wetting properties at the cell walls.

It is generally known that the nematic phase wets more than the isotropic phase [17], but surface treatments can alter the surface tension and therefore the wetting properties at a given surface. A clear example of this is given by type *B* samples. We have seen that the kinetics for the transition on heating (cooling) in these samples is qualitatively similar to the one on cooling (heating) in type *A* and *C* samples. During the heating of sample *B*, at the early stage of the isotropic phase nucleation, on the high temperature side of the sample, we have found isotropic columns in a nematic matrix. This is due to the fact that the polar surfactant CTAB increases the wetting ability of the nematic phase and decreases the contact angle between the nematic and the surface. The isotropic volumes, therefore, increase in size preferentially along the depth of the sample. When cooling the samples *A* and *C*, we find columns of nematic material in an isotropic matrix at the early stage of the nucleation of the nematic phase, but this is mainly related to the reduced vertical thermal gradient in the sample, as described previously. With a larger gradient, in fact, the formation of a NI interface would be more favored.

On cooling type *B* samples the nucleated nematic volumes spread over the surface because of the small contact angle imposed by the CTAB, and a NI interface is therefore formed. We have also found a well-defined NI interface on heating type *A* and *C* samples, but this is again due to the increased vertical temperature gradient we have in this case with respect to cooling measurements, which enforces the formation of the interface even though the isotropic phase ‘‘does not like’’ the surface.

The results clearly show that the presence of CTAB increases the width of the TPCR. One may argue that this is due to the desorption of surfactant molecules from the surface which goes in the LC and acts as a pollutant. This is in contrast with the fact that the transition temperature does not decrease as expected but, in the type *B* sample on the contrary, we have observed a tendency for T_{NI} to increase in the first two or three runs. We do not have at the moment a satisfactory explanation on this particular point. The nondepression of the transition temperature by such possible impurities could, on the other hand, be associated with the fact that CTAB is not a nonmesogenic impurity but it is known to form wormlike micelles and lamellar phases as a function of concentration in water mixture [18].

It is well known that for the study of anomalies of physical quantities close to a first-order phase transition, the presence of a TPCR is a strong limitation since the data in such a region cannot be considered. The larger the TPCR, the poorer the quality of the information we can obtain. The existence of TPCR is known to be associated with the presence of impurities and temperature gradients in the sample as also confirmed by the present results. Regarding impurities we cannot do more than use a carefully purified sample. Also in the case of thermal gradients, a careful choice of the heating stage design and of the ac heating source conditions is advisable. The results we have obtained, however, suggest a possible way out to decrease the influence of at least the lateral temperature gradient. It is clear from the video we have recorded during the measurements that if we reduce the probed area, the lateral variation of the temperature in this area can be reduced. Now, if we consider that the narrowest range value reported for the TPCR is 14 mK, the one obtained using adiabatic scanning calorimetry, and that we can easily reduce it to heated area in our setup, we think that the value of 40 mK value we have for type *A* and *C* samples can be improved. We could eventually obtain a value comparable with the one obtained with high resolution dc techniques which, however, cannot measure all the quantities measured by the present technique. Experiments in this direction are underway and the results will be presented in a forthcoming paper.

It has been suggested [5] that in the TPCR of a first-order phase transition, due to the partial phase conversion (e.g. $N \rightleftarrows I$), the specific heat becomes frequency dependent. This has been associated with the presence of a peak in the phase of the signal of an ac calorimetric technique, which, on the contrary, at a second-order phase transition (frequency independent specific heat) is stated to show a dip [19].

In our case we also find a peak in the signal phase at a first-order phase transition but we have shown that its origin is other than the nonthermodynamic equilibrium condition which is found in a partial phase conversion situation. In fact it is true that in our FD configuration, in a situation of nonthermodynamic equilibrium, a peak should be observed in the signal phase even in an optically opaque, thermally thick, homogeneous sample [20]. However, we think that the close correlation we have found between the presence of a NI interface in the sample and the peak in the phase due to the reflection of the thermal wave at the NI interface makes that hypothesis quite unlikely in our case. We have found a frequency dependence of the PPE signal, but this has nothing to do with the above mentioned partial conversion of one phase into the other and can be simply described in terms of the model for the reflected thermal wave. We have also tried to test the response time needed for a sample at T_{NI} to convert from one phase to the other. This has been done by quickly ramping up and down by small amounts the heating source power. We have found that the appearance of volumes of one phase within the other closely follows the variation of the heating power. This of course does not mean that the conversion is complete, but our feeling is that, combining these results with all the other reported above leads to the conclusion that, at least in our case, this effect does not play any significant role.

V. CONCLUSIONS

In the study of first-order phase transitions, the data in the TPCR are most of the time not considered for two main reasons: the first one is that it is extremely difficult to obtain quantitative information on the physical parameters of a two-phase system and the second is that the kinetics of the nucleation and growth of one phase within the other is also very complicated and dependent on the experimental conditions.

We have tried in this paper to partially overcome these problems at the NI transition of 8CB using an experimental setup which allows the simultaneous high resolution study of thermal parameters behavior and of the sample texture evolution by polarizing microscopy. Using the obtained results we have been able to find a correlation between the PPE signal and the texture of the sample in the TPCR which has been very useful in the study of the kinetics of the phase transition. We have found that, depending on the surface treatment and the thermal gradient in the sample, a NI interface may or may not be present and may move across the sample with increasing or decreasing temperature. This has been possible by analyzing the PPE amplitude and phase on the basis of a simple model which takes into account the contribution of a thermal wave reflected at the interface and correlating it with the observation of the sample texture evolution in the TPCR. We have also found that the kinetics of the transition and therefore the presence of the interface is strongly influenced by the treatments of cell walls and therefore by the wetting properties of the material at such walls. This is particularly evident in the case of CTAB, a polar surfactant used for homeotropic alignment, which significantly increases the wetting ability of the nematic material with respect to the isotropic one and significantly alters the kinetics of the NI transition.

Our experimental setup has allowed an accurate determination of the width of the TPCR. We know that it is influenced by impurities and we have confirmed that it is also affected by the presence of thermal gradients in the sample, as expected. The obtained results, however, give some useful information on possible ways to minimize their influence. We have also found that the presence of polar surfactant, used to induce homeotropic alignment, increases in the width of the TPCR by about a factor of 2. Moreover, though the reason for this is not completely understood, this effect is absent in the case of more ‘‘inert’’ agent used to produce macroscopic alignment, such as quartz deposition in planar samples, for which we have found a TPCR similar to the one found in samples with no surface treatments.

Finally, we have found a frequency dependence on the PPE signal which can be described in terms of the model which takes into account the contribution of the thermal wave reflected at the NI interface to the surface temperature rise of the sample. There is no evidence in our case of an effect due to the a partial conversion of one phase into the other during the heating cycles in the TPCR, which could be the origin of an imaginary part of the specific heat and of its frequency dependence. We believe that in our case the sample is always at the thermodynamic equilibrium also when there is a coexistence between the N and I phases.

[1] J. Thoen, H. Marynissen, and W. Van Dael, Phys. Rev. A **26**, 2886 (1982).

[2] P.K. Mukherjee, J. Phys.: Condens. Matter **10**, 9191 (1998), and references therein.

[3] P.J. Keyes, Phys. Lett. A **67**, 132 (1978).

[4] M.A. Anisimov, *Critical Phenomena in Liquids and Liquid Crystals* (Gordon and Breach Science Publishers, Philadelphia, 1991).

[5] G.S. Iannacchione, C.W. Garland, J.T. Mang, and T.P. Rieker, Phys. Rev. E **58**, 5966 (1998).

[6] T. Börzsönyi and S. Akamatsu, Phys. Rev. E **66**, 051709 (2002).

[7] T. Stoebe and C.C. Huang, Int. J. Mod. Phys. B **9**, 2285 (1995).

[8] P. Korpiun and R. Tilgner, J. Appl. Phys. **51**, 6115 (1980).

[9] F. Mercuri, R. Pizzoferrato, U. Zammit, and M. Marinelli, Appl. Phys. Lett. **81**, 4148 (2002).

[10] M. Marinelli, F.M. Mercuri, U. Zammit, and F. Scudieri, Phys. Rev. E **53**, 701 (1996).

[11] D. Dadarlat, A. Frandas, M. Marinelli, F. Mercuri, and D. Bicanic, Appl. Phys. A: Mater. Sci. Process. **61**, 183 (1995).

[12] M. Marinelli, F. Mercuri, U. Zammit, and F. Scudieri, Phys. Rev. E **58**, 5860 (1998).

[13] A. Mandelis, J. Opt. Soc. Am. A **6**, 298 (1989).

[14] S. Faetti and V. Palleschi, Phys. Rev. A **30**, 3241 (1984).

[15] A. Mandelis and M.M. Zver, J. Appl. Phys. **57**, 4421 (1985).

[16] M. Marinelli, F. Mercuri, S. Foglietta, U. Zammit, and F. Scudieri, Phys. Rev. E **54**, 1604 (1996).

[17] O.A. Gomes, R.C. Falcão, and O.N. Mesquita, Phys. Rev. Lett. **86**, 2577 (2001).

[18] E. Mendes, J. Narayanan, R. Oda, F. Kern, S.J. Kandau, and C. Manohar, J. Phys. Chem. B **101**, 2256 (1997).

[19] H. Haga and C.W. Garland, Phys. Rev. E **56**, 3044 (1997).

[20] B. Büchner and P. Korpiun, Appl. Phys. B: Photophys. Laser Chem. **43**, 29 (1987).